Diffuse neutron scattering study of magnetic correlations in half-doped $La_{0.5}Ca_{0.5-x}Sr_xMnO_3$ manganites ($x=0.1$, 0.3, and 0.4)

I. Dhiman,[1] A. Das,[1,*] R. Mittal,[1] Y. Su,[2] A. Kumar,[1] and A. Radulescu[2]
[1]*Solid State Physics Division, Bhabha Atomic Research Centre, Mumbai 400085, India*
[2]*Juelich Centre for Neutron Science, IFF, Forschungszentrum Juelich, Outstation at FRM II, Lichtenbergstrasse 1, D-85747 Garching, Germany*

(Received 26 October 2009; revised manuscript received 7 January 2010; published 30 March 2010)

The short-range-ordered magnetic correlations have been studied in half-doped $La_{0.5}Ca_{0.5-x}Sr_xMnO_3$ ($x=0.1$, 0.3, and 0.4) compounds by polarized neutron scattering technique. On doping Sr^{2+} for Ca^{2+} ion, these compounds with $x=0.1$, 0.3, and 0.4 exhibit CE-type, mixture of CE-type and *A*-type, and *A*-type antiferromagnetic ordering, respectively. Magnetic diffuse scattering is observed in all the compounds above and below their respective magnetic ordering temperatures and is attributed to magnetic polarons. The correlations are primarily ferromagnetic in nature above T_N, although a small antiferromagnetic contribution is also evident. Additionally, in samples $x=0.1$ and 0.3 with CE-type antiferromagnetic ordering, superlattice diffuse reflections are observed indicating correlations between magnetic polarons. On lowering temperature below T_N, the diffuse scattering corresponding to ferromagnetic correlations is suppressed and the long-range-ordered antiferromagnetic state is established. However, the short-range-ordered correlations indicated by enhanced spin-flip scattering at low Q coexist with long-range-ordered state down to 3 K. In $x=0.4$ sample with *A*-type antiferromagnetic ordering, superlattice diffuse reflections are absent. Additionally, in comparison to $x=0.1$ and 0.3 sample, the enhanced spin-flip scattering at low Q is reduced at 310 K, and as temperature is reduced below 200 K, it becomes negligibly low. The variation in radial correlation function, $g(r)$ with temperature indicates rapid suppression of ferromagnetic correlations at the first nearest neighbor on approaching T_N. Sample $x=0.4$ exhibits growth of ferromagnetic phase at intermediate temperatures (~200 K). This has been further explored using small-angle neutron scattering and neutron depolarization techniques.

DOI: 10.1103/PhysRevB.81.104423 PACS number(s): 75.30.−m, 75.47.Lx, 75.40.−s, 71.38.−k

I. INTRODUCTION

The complex interplay between charge, spin, orbital, and lattice degree of freedom is responsible for the rich phase diagram in doped perovskite $La_{1-x}Ca_xMnO_3$ manganites.[1,2] Neutron scattering studies in doping regime $0.15 \leq x \leq 0.30$ have shown that the transport properties of these materials are controlled by the competition between short-range charge correlations and long-range ferromagnetic double exchange interactions.[3,4] Theoretical understanding enunciates that double exchange interaction alone is insufficient and strong electron-phonon coupling is also required. Origin of this coupling is proposed to be due to lattice polarons and dynamic Jahn-Teller distortions.[5–8] Neutron and x-ray scattering experiments are directly sensitive to both polarons and their correlations and therefore, they make an important contribution to studies of polarons.

In manganites, strong electron-phonon coupling results in the formation of localized charge carriers associated with lattice distortions (polarons) in the paramagnetic insulating regime. Early evidence of polarons has been obtained from transport studies.[9,10] For $La_{0.7}Ca_{0.3}MnO_3$, these polarons take the form of correlations with an ordering of wave vector $\approx(\frac{1}{4},\frac{1}{4},0)$.[11] This type of ordering becomes long range at half doping, having CE-type (charge exchange) antiferromagnetic, charge, and orbitally ordered state with equal number of Mn^{3+} and Mn^{4+} ions.[12,13] In compounds with $x<\frac{1}{2}$, the CE-type antiferromagnetic structure is frustrated and is observed in the insulating state of manganite in the form of nanoscale structural correlations.[4,14–16] The onset of ferromagnetism below T_C (~257 K), leads to melting of these CE-type correlations observed in the insulating regime just above T_C. As a result, no diffuse scattering is observed far below T_C.[4,15–19] Previous x-ray and neutron scattering study on half-doped perovskite manganite $(Nd_{0.125}Sm_{0.875})_{0.52}Sr_{0.48}MnO_3$ and the layered manganite $La_{1.2}Sr_{1.8}Mn_2O_7$ also revealed a direct evidence for the formation of lattice polarons.[20,21] Mellergård *et al.* have reported the absence of local lattice distortions (lattice polarons) below T_C for $La_{1-x}Sr_xMnO_3$ ($x=0.2$ and 0.4) compounds using neutron diffraction and reverse Monte Carlo analysis.[22] They linked the observed distortions above T_C with Mn^{4+} ion, which is different from the Jahn-Teller type associated with the Mn^{3+} ion. Also, the magnetic-moment pair-correlation function calculation gives evidence for short-range magnetic correlations (magnetic polarons). These magnetic polarons are correlated with the local lattice distortions (lattice polarons). The ferromagnetic correlation is associated with shorter Mn-Mn distances and antiferromagnetic correlation with the longer distance.

In this paper, we study the short-range magnetic correlations in $La_{0.5}Ca_{0.5-x}Sr_xMnO_3$ ($x=0.1$, 0.3, and 0.4) series above and below the magnetic ordering temperature by polarized neutron scattering technique. In the parent compound ($x=0$), as a result of 1:1 ratio of Mn^{3+} and Mn^{4+} ions, the charge and orbitally ordered CE-type state is found to be most stable. It exhibits ferromagnetic transition at $T_C \approx 230$ K and a charge and orbitally ordered antiferromagnetic insulating transition at $T_N \approx 170$ K.[23] In the previously reported neutron-diffraction study using unpolarized neu-

 ©2010 The American Physical Society

trons on $La_{0.5}Ca_{0.5-x}Sr_xMnO_3$ ($0.1 \leq x \leq 0.5$) compounds, we have shown the suppression of CE-type antiferromagnetic phase with progressive increase in Sr doping and establishment of ferromagnetic phase.[24] The CE-type antiferromagnetic phase is observed for $x=0.1$, 0.2, and 0.3 samples with antiferromagnetic transition temperatures 150 K, 100 K, and 75 K, respectively. At $x=0.4$, the CE-type antiferromagnetic structure is fully suppressed and *A*-type antiferromagnetic phase is observed with the transition temperature $T_N \approx 200$ K. For $x=0.5$ sample, the *A*-type antiferromagnetic transition temperature is reduced to 125 K and the long-range ferromagnetically ordered phase is established at all temperatures below 310 K. Using polarization analysis techniques, we are able to separate the magnetic diffuse scattering from other contributions such as nuclear and thermal diffuse scattering. As a result, we provide a clear evidence for the presence of magnetic diffuse scattering coexisting with long-range-ordered CE-type and *A*-type antiferromagnetic phase. Additionally, small-angle neutron scattering (SANS) and neutron depolarization measurements have been carried out for sample $x=0.4$ which exhibits ferromagnetic phase in the intermediate temperature regime.

II. EXPERIMENT

The polycrystalline samples $La_{0.5}Ca_{0.5-x}Sr_xMnO_3$ ($x=0.1$, 0.3, and 0.4) were synthesized by conventional solid-state reaction method reported elsewhere. The phase purity of all the samples is confirmed by x-ray and neutron-diffraction techniques reported previously.[24] Polarized neutron-diffraction ($\lambda=4.74$ Å) measurements in the angular range $20° \leq 2\theta \leq 125°$ were carried out on the diffuse neutron scattering spectrometer at FRM-II reactor, at several temperatures between 3 and 310 K. Normal collimators and Beryllium filter for removing $\lambda/2$ contamination were used in the course of the experiment. We have carried out *xyz* polarization analyses to separate the magnetic scattering from nuclear and spin incoherent scattering. SANS measurements ($\lambda=10$ Å) as a function of temperature ($20 \leq T \leq 300$ K) in zero magnetic field for Q range between 10^{-3} and 0.30 $Å^{-1}$ was carried out on SANS instrument (KWS-2) at FRM II reactor. The position-sensitive [two-dimensional (2D)] Anger-type scintillation detector (60×60 cm^2 6Li glass scintillator 1-mm-thick and an array of 8×8 photomultipliers) with a resolution of 0.5×0.5 cm^2 were used to carry out SANS measurements. The 2D raw data were corrected for the scattering from empty can and cryostat windows, the electronic and background noise and calibrated to absolute scale using a plexiglass standard sample. After azimuthal integration of the 2D data, the scattered intensity $I(Q)$ as a function of the scattering vector Q was obtained. Neutron depolarization measurements ($\lambda=1.205$ Å) were carried out on the polarized neutron spectrometer at Dhruva reactor, Bhabha Atomic Research Centre, Mumbai, India, with Cu_2MnAl (1 1 1) as polarizer and Co_2Fe (2 0 0) as analyzer.

III. RESULTS AND DISCUSSION

A. Polarized neutron scattering

The samples studied in the series $La_{0.5}Ca_{0.5-x}Sr_xMnO_3$ ($0 < x \leq 0.3$) crystallize with orthorhombic structure (space group *Pnma*) and $x=0.4$ crystallizes with two orthorhombic phases in the space group *Pnma* and *Fmmm*. The structural and magnetic properties of these samples have been reported previously.[24] In this study, three samples have been chosen which exhibit distinct magnetic structures. The $x=0.1$ compound exhibits CE-type antiferromagnetic spin structure, $x=0.3$ exhibits mixture of CE-type and *A*-type antiferromagnetic structure while, $x=0.4$ undergoes *A*-type antiferromagnetic ordering at low temperatures.[24] The xyz polarization analysis allows us to separate the nuclear and magnetic contributions. All the spin-flip (SF) scattering is purely magnetic in nature. The nonspin-flip (NSF) scattering does not contain magnetic scattering component and has contribution only from nuclear coherent and isotopic incoherent scattering.[25,26] Figure 1 shows a typical diffraction pattern with separated SF and NSF contributions in $x=0.1$ sample at 310 K. The NSF scattering indicating the nuclear Bragg reflections (1 0 1) (0 2 0) at $2\theta \sim 75.5°$ and (2 0 0) (0 0 2) (1 2 1) at $2\theta \sim 123°$ is in agreement with the previously reported structural studies on this compound.[24]

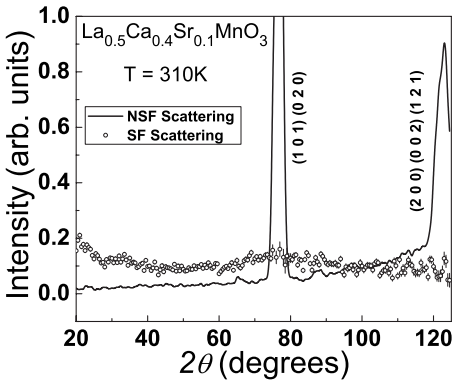

FIG. 1. The nuclear (NSF) and magnetic (SF) contributions to the total scattering for $La_{0.5}Ca_{0.4}Sr_{0.1}MnO_3$ ($x=0.1$) at 310 K from *xyz* polarization analysis.

The SF and NSF scattering for $x=0.1$ sample at 310 K is shown in Fig. 2(a). At this temperature, in the paramagnetic region, magnetic diffuse scattering peak is primarily centered at $2\theta \sim 75.5°$ and a weak superlattice diffuse scattering peak is observed at $\sim 33.5°$, in addition to enhanced scattering at low 2θ values in SF scattering. The broad diffuse scattering peak at $2\theta \sim 75.5°$ is centered around fundamental Bragg reflection (020) (101) (observed for NSF scattering). This peak corresponds to short-range ferromagnetic correlations, as it is observed around the fundamental Bragg reflection indexed as (1 0 1) (0 2 0). At 310 K below $2\theta \sim 30°$, the SF component also shows an enhanced scattering. Existence of enhanced scattering in the SF and the NSF, scattering components have been attributed to the existence of magnetic and lattice polarons, respectively.[27] However, in the present study, enhanced scattering is observed only in the SF component, indicating the existence of magnetic polarons alone. Similarly, the superlattice reflection is attributed to arise from polaron-polaron correlation. The enhanced scattering at low Q is fitted to a Lorentzian-type Q dependence, $I = I_0/[(1/\xi)^2 + Q^2]$, where ξ is the correlation length (Ornstein-Zernike form), as shown in Fig. 2(a). The obtained

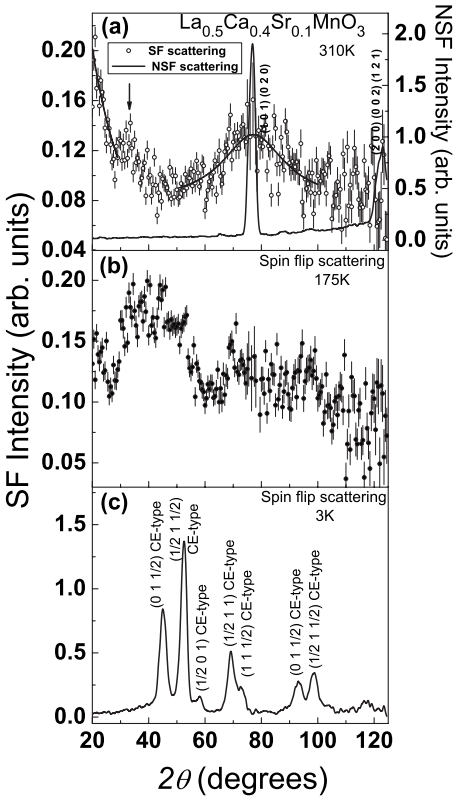

FIG. 2. (a) The SF scattering for sample $La_{0.5}Ca_{0.4}Sr_{0.1}MnO_3$ (x=0.1) at 310 K is shown on left-hand side scale and NSF scattering on right-hand side scale. Arrow indicates the superlattice magnetic diffuse scattering peak centered at $2\theta \sim 33.5°$. Also shown using continuous line in SF scattering is the fit to a Lorentzian-type function described in the text. In (b) SF scattering at 175 K and in (c) at 3 K is shown.

correlation length at 310 K for x=0.1 sample is ~3.4(9) Å, which is on the order of Mn-Mn distance. The diffuse scattering peak evident at $2\theta \sim 33.5°$ indicated by an arrow in Fig. 2(a) is a superlattice peak. The superlattice diffuse peak at $2\theta \sim 33.5°$ is very weak at 310 K. On lowering temperature below 310 K, the superlattice diffuse peak at $2\theta \sim 33.5°$ becomes more pronounced. For x=0.1 sample, the SF scattering at 175 K is shown in Fig. 2(b). However, the broadness of the peak suggests the short-range nature of antiferromagnetic correlations. It is of interest to note that these short-range antiferromagnetic and ferromagnetic correlations are observed at 310 K, which is much above the transition temperature ($T_N \sim 150$ K and $T_C \sim 244$ K) for this compound. Below 175 K, on approaching T_N, the short-range-ordered antiferromagnetic correlations are suppressed with the onset of long-range CE-type antiferromagnetic ordering. Figure 2(c) displays the SF scattering at 3 K indicating the long-range-ordered antiferromagnetic superlattice reflections indexed to a CE-type antiferromagnetic structure reported previously in this compound. Additionally, the absence of SF scattering in the fundamental nuclear reflections rules out the possibility of long-range ferromagnetic ordering coexisting with antiferromagnetic ordering in this sample. The coexistence of the short-range ferromagnetic and antiferromagnetic correlations at 310 K indicates the presence competing magnetic interactions. The temperature dependence of the integrated intensity obtained using a Lorentzian peak shape function fit to the ferromagnetic ($2\theta \sim 33.5°$) and antiferromagnetic ($2\theta \sim 75.5°$) diffuse scattering peaks for sample x =0.1, are shown in Fig. 3. The ferromagnetic diffuse scattering intensity shows a maximum at ~225 K. This maximum is close to the ferromagnetic transition temperature (T_C ~244 K), obtained from previously reported $M(T)$ measurements.[24] On lowering of temperature below 225 K, the short-range-ordered ferromagnetic correlations are suppressed while the antiferromagnetic correlations continue to increase. The onset of long-range antiferromagnetic ordering below 175 K coincides with rapid suppression of short-range ferromagnetic ordering.

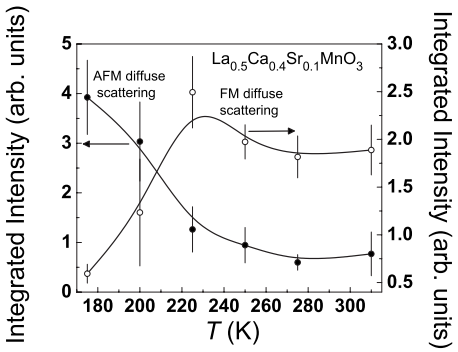

FIG. 3. The temperature dependence of integrated intensity obtained using a Lorentzian function fit to the antiferromagnetic and ferromagnetic diffuse scattering peaks at $2\theta \sim 33.5°$ and ~75.5°, respectively, for sample $La_{0.5}Ca_{0.4}Sr_{0.1}MnO_3$ (x=0.1). The continuous lines are a guide for the eyes.

The SF scattering shown in Fig. 4(a) for $La_{0.5}Ca_{0.2}Sr_{0.3}MnO_3$ (x=0.3) compound displays a superlattice peak centered at $2\theta \sim 33.5°$ and a peak at $2\theta \sim 75.5°$, centered around the fundamental nuclear reflections (1 0 1) (0 2 0), similar to x=0.1 compound. These two peaks correspond to antiferromagnetic and ferromagnetic short-range-ordered correlations, respectively as described for x=0.1 sample. At 275 K, the intensity of superlattice diffuse peak at $2\theta \sim 33.5°$ increases in comparison with 310 K, as evident in Fig. 4(b). Below 150 K, these short-range-ordered antiferromagnetic correlations are suppressed with the onset of long-range ordering. Figure 4(c) displays the SF scattering for x =0.3 sample at 3 K. The superlattice reflections corresponding to long-range-ordered CE-type antiferromagnetic spin structure are observed, in concurrence with our previously reported neutron-diffraction study.[24] In addition, at low temperature, few additional superlattice reflections (at $2\theta \sim 37°$ and ~88°) other than the ones corresponding to CE-type antiferromagnetic spin structure are observed. This antiferromagnetic phase is identified as having an A-type spin structure. We failed to detect this phase in our previous neutron-diffraction studies.[24] Therefore, at low temperature, the magnetic phase of this compound consists of a mixture of CE-type and A-type antiferromagnetic state. Both the magnetic phases have identical transition temperatures (T_N). The short-range-ordered ferromagnetic interactions are similar to x=0.1 sample and no long-range ferromagnetic ordering is observed down to 3 K.

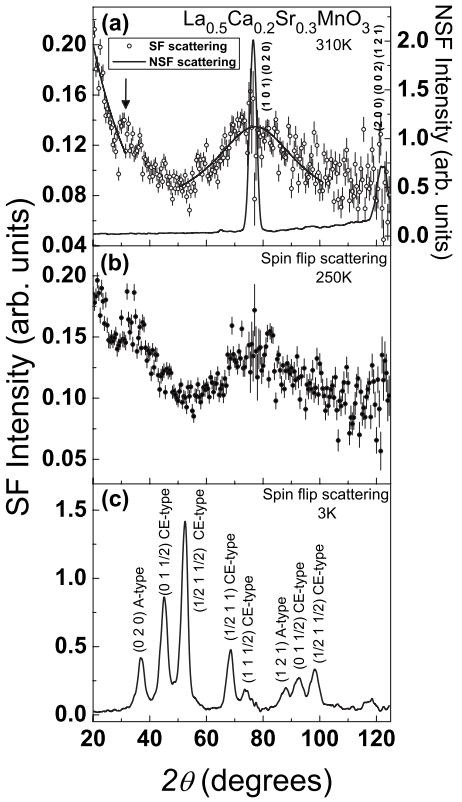

FIG. 4. (a) The SF scattering for sample $La_{0.5}Ca_{0.2}Sr_{0.3}MnO_3$ (x=0.3) at 310 K is shown on left-hand side scale and NSF scattering, on right-hand side scale, continuous line in SF scattering is the fit to a Lorentzian-type function described in the text. Arrow indicates the superlattice diffuse scattering peak centered at $2\theta \sim 33.5°$. In (b) SF scattering at 250 K and in (c) at 3 K is shown.

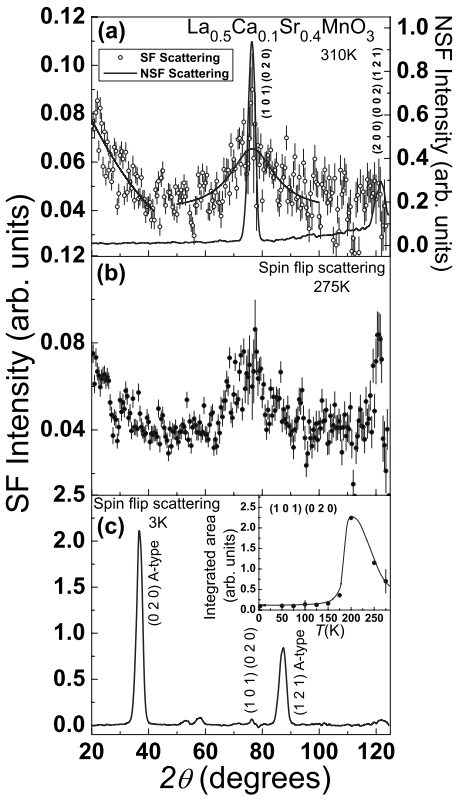

FIG. 5. (a) The SF scattering for sample $La_{0.5}Ca_{0.1}Sr_{0.4}MnO_3$ (x=0.4) at 310 K is shown on left-hand side scale and NSF scattering, on right-hand side scale, continuous line in SF scattering shows the fit to a Lorentzian function. Arrow indicates the superlattice diffuse scattering peak centered at $2\theta \sim 33.5°$. In (b) SF scattering at 275 K and in (c) at 3 K is shown. The inset in (c) is the integrated intensity of the diffuse Bragg peak (1 0 1) (0 2 0) at $2\theta \approx 75.5°$.

The SF scattering at 310 K for x=0.4 sample displayed in Fig. 5(a) provides evidence of diffuse ferromagnetic correlations and enhanced scattering at low 2θ values. This sample with A-type antiferromagnetic ordering does not display the superlattice diffuse reflection at $2\theta \sim 33.5°$, which is observed in x=0.1 and 0.3 compounds having dominant CE-type antiferromagnetic spin structure. The diffuse ferromagnetic scattering peak at $2\theta \sim 75.5°$, observed in Figs. 5(a) and 5(b) is similar to x=0.1 and 0.3 compounds. Figure 5(c) exhibits the SF scattering (purely magnetic scattering) at 3 K. Below 250 K, well-defined superlattice Bragg reflections are observed indicating the onset of long-range-ordered A-type antiferromagnetic structure. The superlattice reflections corresponding to long-range-ordered A-type antiferromagnetic phase are evident in Fig. 5(c). Integrated intensity of the ferromagnetic diffuse peak centered at $2\theta \sim 75.5°$ is shown in the inset of Fig. 5(c). This peak exhibits a maximum at 200 K, with the establishment of long-range-ordered ferromagnetic interactions between 250 and 150 K. Below 150 K, this ferromagnetic phase is suppressed. This behavior is in agreement with the maximum in magnetization reported earlier and minimum in neutron depolarization (Fig. 10) measurements discussed subsequently. Also, our neutron-diffraction measurements reported earlier display similar maximum in integrated intensity versus temperature plot for (1 0 1) (0 2 0) reflection.[24]

From the full width at half maximum (ΔQ) of the diffuse scattering centered at $2\theta \sim 75.5°$, the size of the short-range-ordered regions is estimated. ΔQ for the ferromagnetic diffuse scattering peak was estimated by fitting it to a Lorentzian peak shape function. The Lorentzian fit for x=0.1, 0.3, and 0.4 compounds is shown in Figs. 2(a), 4(a), and 5(a), respectively. The correlation length, ξ ($=2\pi/\Delta Q$) at 310 K has values of 13(2) Å, 10(1) Å and 15(2) Å for x=0.1, 0.3, and 0.4 samples, respectively. No significant change in ξ is observed with variation in temperature.

In Fig. 6, the temperature dependence of magnetic diffuse scattering intensity at Q=0.46 $Å^{-1}$ ($2\theta \approx 20°$) for $La_{0.5}Ca_{0.5-x}Sr_xMnO_3$ series with x=0.1, 0.3, and 0.4 is displayed. For x=0.1 and 0.3 samples, similar temperature dependence of magnetic diffuse scattering intensity is observed. The short-range-ordered antiferromagnetic correlation in x=0.1 and 0.3 compounds coexist with the long-range CE-type antiferromagnetic ordering at the lowest temperature of 3 K. However, for x=0.4 composition, these short-range-ordered antiferromagnetic correlations are much reduced as compared to x=0.1 and 0.3 compounds.

The evidence of diffuse scattering in polarization analysis measurements of these samples indicates the existence of magnetic polarons above the transition temperature. Absence of diffuse scattering in the nuclear coherent scattering (NSF

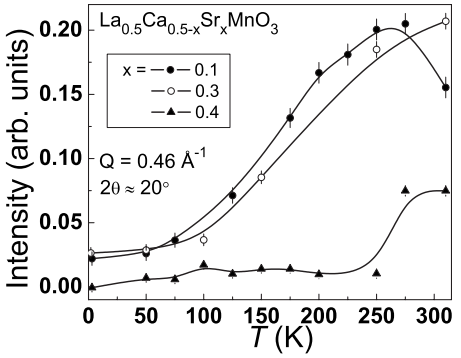

FIG. 6. Evolution of neutron scattering intensity as a function of temperature at $Q=0.46$ Å^{-1} ($2\theta \approx 20°$) for $La_{0.5}Ca_{0.5-x}Sr_xMnO_3$ series, where $x=0.1$, 0.3, and 0.4. The continuous lines are a guide for the eyes.

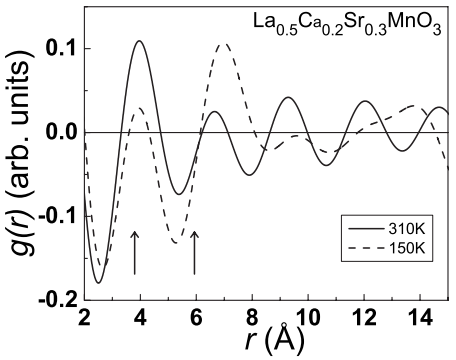

FIG. 8. Radial correlation function $g(r)$ for $La_{0.5}Ca_{0.2}Sr_{0.3}MnO_3$ ($x=0.3$) at 310 and 150 K. Arrows indicate the two nearest-neighbor bond distances for Mn sublattice.

scattering) component, indicate the absence of lattice polarons. Similar study using neutron polarization analysis technique on half-doped $Nd_{0.5}Pb_{0.5}MnO_3$ compound has been reported by Clausen *et al.*[28] Strong diffuse magnetic scattering is observed above T_C, attributed to magnetic polarons (SF scattering) while lattice polarons (NSF scattering) are not observed. Therefore, short-range-ordered antiferromagnetic correlation are visible above the transition temperature and are precursors to CE-type antiferromagnetic phase. This is distinct from similar studies reported in ferromagnetic compound $La_{0.7}Ca_{0.3}MnO_3$ where short-range-ordered CE-type polarons are found to exist above T_C in the insulating state.[14]

Mellergård *et al.*[22] have associated the ferromagnetic correlations with the shorter Mn-Mn distances and antiferromagnetic correlation with longer distances. To obtain a similar behavior on the antiferromagnetic and ferromagnetic correlations as a function of distance, we have calculated the radial correlation function, $g(r)$. The $g(r)$ is obtained from the SF scattering data, using the following expression:[29]

$$g(r) = \int_{Q_1}^{Q_h} I_{\mathrm{mag}}(Q) f(Q)^{-2} Q \sin(Qr) dQ, \qquad (1)$$

where, Q ($=4\pi \sin\theta/\lambda$) is the scattering vector, $I_{\mathrm{mag}}(Q)$ is the magnetic scattering intensity, and $f(Q)$ is the magnetic scattering form factor. Assuming that the interactions are isotropic, $g(r)$ is related to spin-spin correlation function by the following expression:[30]

$$g(r) = \frac{1}{S(S+1)} \sum_{r'} \langle S_0 \cdot S_{r'} \rangle \cdot \delta(|r| - |r'|). \qquad (2)$$

This expression is a sum of spin-spin correlation function at distance r. Figures 7–9 show the variation in $g(r)$ calculated for various temperatures for sample $x=0.1$, 0.3, and 0.4, respectively. It is apparent from these figures that there is a strong change in the average character of the short-range magnetic interactions with nearest neighbors, when approaching the transition temperature from the higher temperature. Figure 7 shows the radial correlation function $g(r)$ at 310, 200, 175, and 125 K for $La_{0.5}Ca_{0.4}Sr_{0.1}MnO_3$ ($x=0.1$) sample, with first to fifth nearest-neighbor Mn pairs indicated by arrow. Well above the ferromagnetic transition temperature, the Mn-Mn pairs which are nearest neighbors (~4 Å) build up ferromagnetic correlations within the paramagnetic matrix, as can be inferred from the positive value of $g(r)$ for small r. This behavior is also evident in Fig. 2, where diffuse scattering is observed at $2\theta \sim 75.5°$, indicative of short-range-ordered ferromagnetic correlations. In addition, for Mn-Mn pairs located at next-nearest-neighbor distances ~5.4 Å, $g(r)$ shows negative value, as shown in Fig.

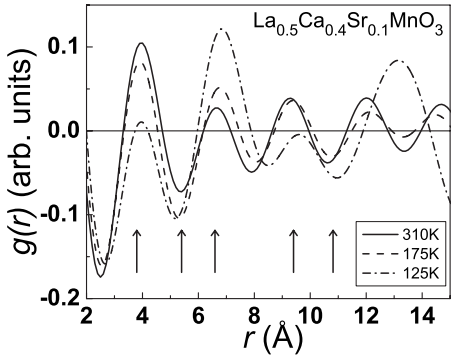

FIG. 7. Radial correlation function $g(r)$ for $La_{0.5}Ca_{0.4}Sr_{0.1}MnO_3$ ($x=0.1$) at 310, 175, and 125 K. Arrows indicate the five nearest-neighbor bond distances for Mn sublattice.

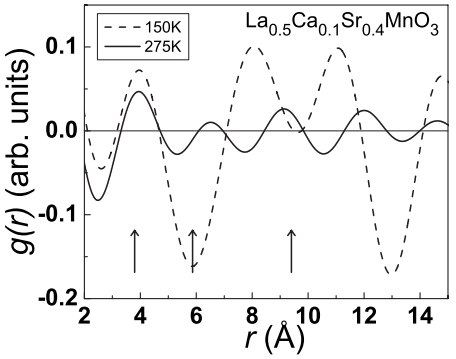

FIG. 9. Radial correlation function $g(r)$ for $La_{0.5}Ca_{0.1}Sr_{0.4}MnO_3$ ($x=0.4$) at 275 and 150 K. Arrows indicate the three nearest-neighbor bond distances for Mn sublattice.

7. This suggests the existence of magnetic correlations of an antiferromagnetic character. The temperature evolution of these correlations for $x=0.1$ sample, show that the ferromagnetic correlations at the first nearest-neighbor distance are strongly suppressed as temperature is reduced. On the other hand, the antiferromagnetic correlations do not exhibit appreciable change with temperature. Figure 8 displays $g(r)$ for $x=0.3$ sample at 310 and 150 K. Arrows indicate the first two nearest-neighbor bond distance for Mn pairs. Similar to $x=0.1$ sample, the positive value of $g(r)$ for nearest-neighbor Mn-Mn pairs and the negative value of $g(r)$ for next-nearest-neighbor Mn-Mn pairs indicate the existence of ferromagnetic and antiferromagnetic magnetic correlations, respectively. Figure 9 shows the radial correlation function $g(r)$ for $La_{0.5}Ca_{0.1}Sr_{0.4}MnO_3$ ($x=0.4$) sample at 275 and 150 K. The three nearest-neighbor bond distances for Mn pairs are indicated by arrows. In this sample, $g(r)$ has a positive value for Mn pairs separated by distances ~3.8 Å. This indicates that nearest-neighbor correlations are ferromagnetic in nature. On reducing temperature, the ferromagnetic correlations does not change appreciably. The $g(r)$ for the next-nearest-neighbor Mn-Mn pairs (~6 Å) is negative, indicating the antiferromagnetic nature of the correlations. On reducing temperature below T_N, the antiferromagnetic correlations are strongly enhanced while the ferromagnetic correlations at the first nearest-neighbor distance are only moderately influenced. This behavior may be correlated with the *A*-type antiferromagnetic ordering observed in this compound, where antiferromagnetic coupling exists between ferromagnetic planes.

B. Neutron depolarization

Unlike, $x=0.1$ and 0.3 compounds, where no evidence of long-range ferromagnetic ordering is observed, sample $x=0.4$ exhibits an unusual behavior of increase in ferromagnetic behavior between 150 and 250 K [as shown by the increase in SF intensity of the fundamental Bragg reflections (101) (020) in the inset of Fig. 5(c)]. This behavior is further studied using neutron depolarization. Neutron depolarization is a technique suitable for the detection of magnetic inhomogeneities on mesoscopic length scale ranging from 1000 Å to several microns. In the present study, we have measured flipping ratio R (ratio of the transmitted intensities for two spin states of the incident neutron spin) which is a measure of the transmitted-beam polarization. R is expressed in the form[31,32]

$$R = \frac{1 - P_i D P_A}{1 + (2f - 1) P_i D P_A},$$

where, P_i is the incident-beam polarization, P_A is the efficiency of the analyzer crystal, f is the rf flipper efficiency, and D is the depolarization coefficient. In the absence of any depolarization in sample, $D=1$. P_iD is thus the transmitted-beam polarization.

Figure 10 shows the temperature dependence of transmitted neutron-beam polarization (P) for sample $La_{0.5}Ca_{0.1}Sr_{0.4}MnO_3$ ($x=0.4$), with $H=50$ Oe, under zero-field-cooled conditions. For this sample, polarization remains

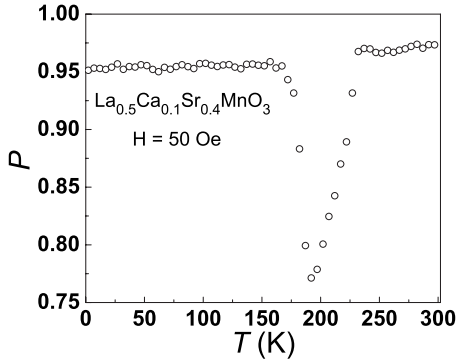

FIG. 10. Temperature dependence of transmitted neutron-beam polarization (P) for sample $La_{0.5}Ca_{0.1}Sr_{0.4}MnO_3$ ($x=0.4$) in $H=50$ Oe.

constant up to ~232 K. Below 232 K, polarization decreases rapidly, reaching a minimum at ~180 K. As temperature is reduced further, polarization again increases almost reaching the same value as in the paramagnetic state. The decrease in polarization below 232 K indicates the onset of ferromagnetic ordering. This behavior correlates well with our previously reported magnetization $M(T)$ and neutron-diffraction study on this compound.[24] The rapid suppression of the depolarization signal below 180 K indicates the reduction in domain size (δ) and/or domain magnetization (B). This behavior correlates with the observation of a maximum at ~200 K in integrated intensity of SF scattering peak (1 0 1) (0 2 0) for this sample, shown in inset of Fig. 5(c). The reduction in ferromagnetic nature in antiferromagnetic phase (with *A*-type spin structure) below 180 K is a consequence of competing interactions between antiferromagnetic and ferromagnetic interactions.

An estimate of domain size in the ferromagnetic region is obtained using the expression

$$P_f = P_i \exp[-\alpha(d/\delta)]\langle\phi_\delta\rangle^2,$$

where, P_f and P_i are the transmitted-beam and incident-beam polarization, respectively, α is a dimensionless parameter $=1/3$, d is the sample thickness, δ is a typical domain length, and the precession angle $\phi_\delta=(4.63\times10^{-10}$ Oe^{-1} Å$^{-2})\lambda\delta B$.[33,34] The domain magnetization, B is obtained from the bulk magnetization. This expression is valid in the limit where domains are randomly oriented and the Larmor phase of neutron spin due to the internal magnetic field of sample $<2\pi$ over a typical domain length scale. Our measurements were carried out in low field far away from the saturation field and therefore satisfy the assumption of this model. The estimated domain size in the present sample at $T=2$ K is ~0.8 μm.

The depolarization measurements were also performed for sample $x=0.1$ and 0.3. However, no change in transmitted-beam polarization was observed down to lowest temperature of 2 K. This is in agreement with the SF scattering measurements on these samples where no evidence of enhancement in the intensity of the fundamental Bragg reflections (101) (020) is observed. Thus we rule out presence of ferromag-

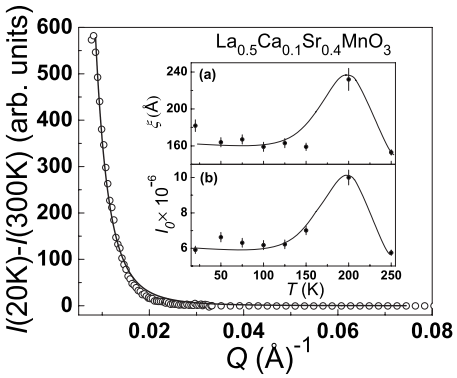

FIG. 11. SANS intensity (open circles) as a function of Q (Å^{-1}) for sample $La_{0.5}Ca_{0.1}Sr_{0.4}MnO_3$ (x=0.4). The continuous line is a squared Lorentzian fit, as described in the text. The inset displays the temperature dependence of (a) correlation length (ξ) and (b) Lorentzian amplitude I_0.

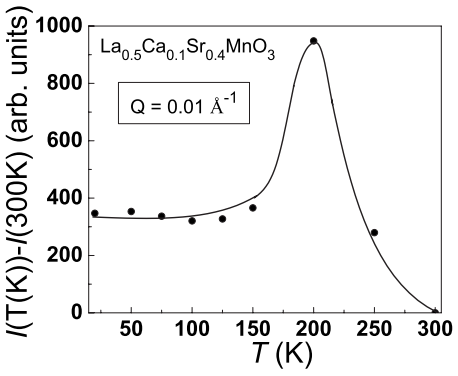

FIG. 12. SANS intensity as a function of temperature at Q =0.01 Å^{-1} for $La_{0.5}Ca_{0.1}Sr_{0.4}MnO_3$ (x=0.4) sample. The continuous line is a guide for the eyes.

netic correlations in the CE-type antiferromagnetic phase of samples x=0.1 and 0.3.

C. Small-angle neutron scattering

The evolution of magnetic scattering intensity $[I(20)\text{-}I(300)]$ as a function of Q ($0.0073 \leq Q \leq 0.080$ Å^{-1}) for $La_{0.5}Ca_{0.1}Sr_{0.4}MnO_3$ (x=0.4) compound is shown in Fig. 11. The Q range in which measurements were carried out corresponds to length scale of 40–1000 Å. This figure $[I(T)\text{-}I(300)]$ is representative for all the temperatures in the range $20 \leq T < 300$ K, To estimate the Q dependence of the magnetic scattering in SANS, intensity at each temperature was subtracted from data at 300 K, taken as the background intensity. The pure magnetic scattering intensity $[I(20\text{ K})\text{-}I(300\text{ K})]$ thus obtained, in the Q range 0.007–0.08 Å is best described by squared Lorentzian-type function, $I=I_0/[(1/\xi)^2+Q^2]^2$, where ξ is the spin-spin correlation length and I_0 is Lorentz amplitude related to the bulk susceptibility. The temperature dependence of fitting parameters is shown in the inset of Fig. 11. The correlation length varies from 123(4) Å at 20 K to 153(3) Å at 250 K, exhibiting a maximum at 200 K having a value of 232(12) Å. The ferromagnetic correlation length obtained from SANS measurements is much smaller than the size of the domains obtained from depolarization measurements due to the difference in length scales at which the two techniques probe. Such differing values from the two measurements have been reported previously.[35,36] The Lorentz amplitude I_0 also behaves in a similar manner, with a maximum at 200 K, following a behavior similar to $M(T)$, reported previously. The squared Lorentzian behavior in SANS intensity is expected for static cluster scattering. Debye *et al.* reported from theoretical study that a squared Lorentzian-type function would be observed for an array of random shapes, sizes, and distribution in a solid matrix.[37,38] In our analysis, additional Lorentzian term which describes a critical scattering was not necessary to fit the data.[39]

Figure 12 shows the temperature dependence of the scattered neutron intensity at Q value 0.01 Å^{-1} for sample $La_{0.5}Ca_{0.1}Sr_{0.4}MnO_3$ (x=0.4). At a length scales, of ~63 nm (Q=0.01 Å^{-1}), intensity as a function of temperature displays a maximum at 200 K. This coincides with the maximum in magnetization reported earlier and minimum in transmitted neutron-beam polarization P (Fig. 10) (~180 K). This suggests that the nature of this enhancement is magnetic. In our previous neutron-diffraction experiments, we observed a maximum in integrated intensity versus temperature plot for (1 0 1) (0 2 0) nuclear peaks at ~200 K, indicating the presence of ferromagnetic interactions.

IV. CONCLUSION

The study of magnetic correlations in $La_{0.5}Ca_{0.5-x}Sr_xMnO_3$ (x=0.1, 0.3, and 0.4) above and below the ordering temperature is carried out using polarized neutron scattering, neutron depolarization, and small-angle neutron scattering techniques. On doping Sr^{2+} ion for Ca^{2+} ion these compounds x=0.1, 0.3, and 0.4 exhibit CE-type, mixture of CE-type and A-type, and A-type antiferromagnetic ordering, respectively. Magnetic diffuse scattering is observed in all the compounds above and below their respective magnetic ordering temperatures and is attributed to magnetic polarons. The correlations are primarily ferromagnetic in nature above T_N, although a small antiferromagnetic contribution is also evident. Additionally, in samples x=0.1 and 0.3 with CE-type antiferromagnetic ordering superlattice diffuse reflections are observed indicating correlations between magnetic polarons. On lowering temperature below T_N, the diffuse scattering corresponding to ferromagnetic correlations is suppressed and the long-range-ordered antiferromagnetic state is established. However, the short-range-ordered correlations indicated by enhanced spin-flip scattering at low Q coexist with long-range-ordered state down to 3 K. In x =0.4 sample with A-type antiferromagnetic order superlattice diffuse reflections are absent. The enhanced spin-flip scattering at low Q is much reduced at 310 K, in comparison to x =0.1 and 0.3 sample. As temperature is decreased below 200 K, it becomes negligibly small. The variation in radial

correlation function, $g(r)$ with temperature indicates rapid suppression of ferromagnetic correlations at the first nearest neighbor on approaching T_N. Sample $x=0.4$ exhibits growth of ferromagnetic phase in intermediate temperatures. This has been further explored using SANS and neutron depolarization techniques and allow us to estimate a spin-spin correlation length (ξ) of ~232(12) Å and a domain size of ~0.8 μm at 200 K.

*adas@barc.gov.in

[1] C. N. R. Rao and B. Raveau, *Colossal Magnetoresistance, Charge Ordering, and Related Properties of Manganese Oxides* (World Scientific, Singapore, 1998).

[2] M. Pissas and G. Kallias, Phys. Rev. B **68**, 134414 (2003).

[3] C. Zener, Phys. Rev. **82**, 403 (1951).

[4] P. Dai, J. A. Fernandez-Baca, N. Wakabayashi, E. W. Plummer, Y. Tomioka, and Y. Tokura, Phys. Rev. Lett. **85**, 2553 (2000).

[5] A. J. Millis, B. I. Shraiman, and R. Mueller, Phys. Rev. Lett. **77**, 175 (1996).

[6] H. Röder, J. Zang, and A. R. Bishop, Phys. Rev. Lett. **76**, 1356 (1996).

[7] G.-m. Zhao, K. Conder, H. Keller, and K. A. Muller, Nature (London) **381**, 676 (1996).

[8] G. Khaliullin and R. Kilian, Phys. Rev. B **61**, 3494 (2000).

[9] M. F. Hundley, M. Hawley, R. H. Heffner, Z. X. Jia, J. J. Neumeier, J. Tesmer, J. D. Thompson, and X. D. Wu, Appl. Phys. Lett. **67**, 860 (1995).

[10] M. Jaime, H. T. Hardner, M. B. Salamon, M. Rubinstein, P. Dorsey, and D. Emin, Phys. Rev. Lett. **78**, 951 (1997).

[11] J. W. Lynn, D. N. Argyriou, Y. Ren, Y. Chen, Y. M. Mukovskii, and D. A. Shulyatev, Phys. Rev. B **76**, 014437 (2007).

[12] E. O. Wollan and W. C. Koehler, Phys. Rev. **100**, 545 (1955).

[13] J. B. Goodenough, Phys. Rev. **100**, 564 (1955).

[14] C. P. Adams, J. W. Lynn, Y. M. Mukovskii, A. A. Arsenov, and D. A. Shulyatev, Phys. Rev. Lett. **85**, 3954 (2000).

[15] J. W. Lynn, C. P. Adams, Y. M. Mukovskii, A. A. Arsenov, and D. A. Shulyatev, J. Appl. Phys. **89**, 6846 (2001).

[16] C. S. Nelson, M. v. Zimmermann, Y. J. Kim, J. P. Hill, D. Gibbs, V. Kiryukhin, T. Y. Koo, S.-W. Cheong, D. Casa, B. Keimer, Y. Tomioka, Y. Tokura, T. Gog, and C. T. Venkataraman, Phys. Rev. B **64**, 174405 (2001).

[17] J. W. Lynn, R. W. Erwin, J. A. Borchers, Q. Huang, A. Santoro, J.-L. Peng, and Z. Y. Li, Phys. Rev. Lett. **76**, 4046 (1996).

[18] J. W. Lynn, R. W. Erwin, J. A. Borchers, A. Santoro, Q. Huang, J.-L. Peng, and R. L. Greene, J. Appl. Phys. **81**, 5488 (1997).

[19] C. P. Adams, J. W. Lynn, V. N. Smolyaninova, A. Biswas, R. L. Greene, W. Ratcliff, S.-W. Cheong, Y. M. Mukovskii, and D. A. Shulyatev, Phys. Rev. B **70**, 134414 (2004).

[20] S. Shimomura, N. Wakabayashi, H. Kuwahara, and Y. Tokura, Phys. Rev. Lett. **83**, 4389 (1999).

[21] L. Vasiliu-Doloc, S. Rosenkranz, R. Osborn, S. K. Sinha, J. W. Lynn, J. Mesot, O. H. Seeck, G. Preosti, A. J. Fedro, and J. F. Mitchell, Phys. Rev. Lett. **83**, 4393 (1999).

[22] A. Mellergård, R. L. McGreevy, and S. G. Eriksson, J. Phys.: Condens. Matter **12**, 4975 (2000).

[23] P. G. Radaelli, D. E. Cox, M. Marezio, and S.-W. Cheong, Phys. Rev. B **55**, 3015 (1997).

[24] I. Dhiman, A. Das, P. K. Mishra, and L. Panicker, Phys. Rev. B **77**, 094440 (2008).

[25] R. M. Moon, T. Riste, and W. C. Koehler, Phys. Rev. **181**, 920 (1969).

[26] J. Schweizer, in *Neutron Scattering from Magnetic Materials*, edited by T. Chatterji (Elsevier B.V., Amsterdam, 2006).

[27] T. Ersez, J. C. Schulz, and T. R. Finlayson, Mater. Forum **27**, 80 (2004).

[28] K. N. Clausen, W. Hayes, D. A. Keen, R. M. Kusters, R. L. McGreevy, and J. Singleton, J. Phys.: Condens. Matter **1**, 2721 (1989).

[29] E. F. Bertaut and P. Burlet, Solid State Commun. **5**, 279 (1967).

[30] J. N. Reimers, J. E. Greedan, R. K. Kremer, E. Gmelin, and M. A. Subramanian, Phys. Rev. B **43**, 3387 (1991).

[31] S. M. Yusuf and L. M. Rao, Pramana **47**, 171 (1996).

[32] L. M. Rao, S. M. Yusuf, and R. S. Kothare, Indian J. Pure Appl. Phys. **30**, 276 (1992).

[33] G. Halpern and T. Holstein, Phys. Rev. **59**, 960 (1941).

[34] R. W. Erwin, J. Appl. Phys. **67**, 5229 (1990).

[35] T. Sato, T. Ando, T. Watanabe, S. Itoh, Y. Endoh, and M. Furusaka, Phys. Rev. B **48**, 6074 (1993).

[36] S. V. Grigoriev, S. V. Maleyev, A. I. Okorokov, and V. V. Runov, Phys. Rev. B **58**, 3206 (1998); V. V. Runov, Physica B **297**, 234 (2001).

[37] P. Debye, H. R. Anderson, and H. Brumberger, J. Appl. Phys. **28**, 679 (1957).

[38] M. L. Spano and J. J. Rhyne, J. Appl. Phys. **57**, 3303 (1985).

[39] J. M. De Teresa, M. R. Ibarra, P. A. Algarabel, C. Ritter, C. Marquina, J. Blasco, J. García, A. del Moral, and Z. Arnold, Nature (London) **386**, 256 (1997).